

# Beyond the $1/T_p$ limit: two-photon-excited fluorescence using pulses as short as sub-10-fs

Shuo Pang  
Alvin T. Yeh  
Chao Wang  
Kenith E. Meissner

Texas A&M University  
Department of Biomedical Engineering  
337 Zachry Engineering Center  
3120 TAMU  
College Station, Texas 77843

**Abstract.** Two-photon-excited fluorescence and second-harmonic generation are characterized as a function of laser pulse duration as short as sub-10-fs. A comparative study is performed where pulse duration is varied by introducing dispersion, as reported previously, and by tailoring pulse spectral width and minimizing its time-bandwidth product (transform-limited pulses). Experimental data and calculations show that characterizing a two-photon signal with the two schemes to vary pulse duration measures different phenomena. Two-photon signal characterization using dispersion-broadened pulses measures only the effect of chirp on the pulse two-photon-excitation spectrum and is independent of molecular response. Transform-limited pulses are used to measure the dependence of two-photon signal generation on pulse duration. Calculations show that deviation from the  $1/T_p$  relationship would be expected as the transform-limited pulse spectral width approaches the molecular two-photon absorption linewidth and exhibits asymptotic behavior for pulse spectral widths 10 times greater than the absorption linewidth. Experimental measurements are consistent with the predicted behavior. The impact of using ultrashort laser pulses on the performance characteristics of nonlinear optical microscopy is discussed. © 2009 Society of Photo-Optical Instrumentation Engineers. [DOI: 10.1117/1.3253388]

Keywords: multiphoton microscopy; two-photon-excited fluorescence; ultrashort laser pulse.

Paper 09169RRR received Apr. 29, 2009; revised manuscript received Aug. 24, 2009; accepted for publication Aug. 26, 2009; published online Oct. 30, 2009.

## 1 Introduction

Nonlinear optical microscopy (NLOM) utilizes femtosecond laser pulses to render thin, microscopic images from within thick, intact tissues without fixing or sectioning. The nonlinear dependence on incident laser intensity localizes signal generation to the focus of the NLOM system, which eliminates the need for confocal pinholes to discriminate against out-of-focus light and simplifies signal detection configurations for image rendering. It has been suggested that NLOM performance (nonlinear optical signal generation, imaging depth, etc.) may be improved by optimizing pulse shape<sup>1</sup> and/or using shorter pulse durations.<sup>2-5</sup> This study characterizes the use of ultrashort duration pulses as short as sub-10-fs with 120-nm full-width at half-maximum (FWHM).

For a given pulse spectrum, nonlinear optical signal generation, in particular, fluorescence following two-photon absorption (TPA), or two-photon-excited fluorescence (TPEF), is maximized when using that spectrum's transform-limited (or minimum time duration) pulse.<sup>2-4</sup> This holds true for the nonresonant case, where there are no real intermediates between the ground and excited states.<sup>6</sup> With an assumed pulse

shape, it can be shown that the two-photon transition probability will increase in proportion to  $1/T_p$ , where  $T_p$  is the transform-limited pulse duration, in the limit of invariant absorption cross section over the entire pulse excitation spectrum.<sup>2</sup> Deviations from the  $1/T_p$  relationship would be expected for shorter pulses when the pulse (two-photon-excitation) spectral width approaches and even exceeds that of the molecular TPA profile. This regime has not been explored or characterized experimentally, but TPEF as a function of pulse duration would be expected to vary depending on the molecular absorption profile with which the laser pulse interacts.

In experiments to characterize TPEF dependence on pulse duration, two different methods were used. TPEF intensity was measured as a function of pulse duration in which (1) the pulse spectrum remained constant while changing phase (chirp)<sup>2,4</sup> and, more recently, (2) the phase remained constant (transform-limited) while changing the pulse spectrum.<sup>5</sup> A laser pulse with a given duration in scheme 1 has different phase and spectrum than one of the same duration in scheme 2 (except for the initial transform-limited pulse). For scheme 1, a prism pair was inserted into the path of 20-<sup>4</sup> and 60-fs pulses<sup>2</sup> to produce longer duration pulses by introducing dispersion. Under this scheme, the dependence of second-order

Address all correspondence to: Alvin Yeh, Prof., Texas A&M University, Department of Biomedical Engineering, 337 Zachry Engineering Center, 3120 TAMU, College Station, TX 77843. Tel: 979-845-5468; Fax 979-845-4450; E-mail: ayeht@tamu.edu

signal (TPEF and second-harmonic generation) was either (1) found to deviate from (with a  $T_p^{-0.85}$  relationship<sup>4</sup>) or (2) short temporal duration data were omitted to recover the  $1/T_p$  relationship.<sup>2</sup> For scheme 2, the spectral width was controlled, the time-bandwidth product minimized, and the pulse was used to measure TPEF as a function of pulse duration from  $\sim 100$  to  $\sim 15$  fs.<sup>5</sup> Deviation in the dependence of TPEF intensity from  $1/T_p$  was found for the shortest-duration (broadest-bandwidth) pulses, but no characterization of the fluorophore was given to enable investigation into the cause. A major goal of our study is to experimentally characterize TPEF dependence on pulse duration in samples with different TPA cross sections.

Here, we explore TPEF in three common biological dyes (FITC, TRITC, and Texas Red) and frequency-invariant second-order signal using transform-limited pulses ranging from sub-10 to 43 fs in duration. Two-photon transition probabilities are calculated for these dyes using measured two-photon photoluminescence excitation spectra (2PES) and experimental pulse spectra to compare with measured TPEF intensities. In addition, transition probabilities are calculated as a function of Gaussian pulse width to predict how TPEF would vary as a function of pulse duration. For comparison to earlier work, the TPEF signal from all samples is also characterized by dispersion-broadened sub-10-fs pulses. Both experiments and calculations confirm that the dependence of TPEF on pulse duration is revealed when characterized using scheme 2 as opposed to using chirped pulses of scheme 1.

## 2 Materials and Methods

The 2PES of each dye was measured using a tunable Ti:Al<sub>2</sub>O<sub>3</sub> oscillator (Mira 900F, Coherent) pumped by a frequency-doubled Nd:YVO<sub>4</sub> solid state laser (Verdi V10, Coherent). The central wavelength of 170-fs pulses was tuned between 700 and 890 nm in 10-nm increments. Laser pulses were focused into a 1-cm pathlength, B270 cuvette containing dye solution using a parabolic mirror (50-mm focal length). FITC, TRITC (Sigma Aldrich), and Texas Red (Sulforhodamine 101, TXred; Molecular Probes) were dissolved in their appropriate solvents (100  $\mu$ M) without further purification from the vendor. TPEF spectra were detected at a right angle to the excitation beam by a thermoelectrically cooled detector array and spectrometer (2300i, Roper Scientific). A 1-mm-thick BG39 (Schott) glass filter was used to reject scattered laser light.

FITC, TRITC, and TXred were selected for study because their 2PES profiles (points) were well centered, to the low- and high energy side of the sub-10-fs pulse two-photon excitation spectrum (dotted line), respectively (see Fig. 1). The two-photon excitation spectrum of the pulse was calculated assuming constant phase (transform-limited) as,

$$T(\omega) = \left| \int_0^\infty E(\omega/2 + \Omega)E(\omega/2 - \Omega)d\Omega \right|^2, \quad (1)$$

where  $E(\omega)$  is the pulse electric field in the frequency domain, and  $\Omega$  is an iterative variable that ensures integration over all possible combinations of frequency components such that  $\omega = \omega_a + \omega_b$ . A sum of Gaussians was used to fit the 2PES line shapes, as shown for each of the dyes (solid line in

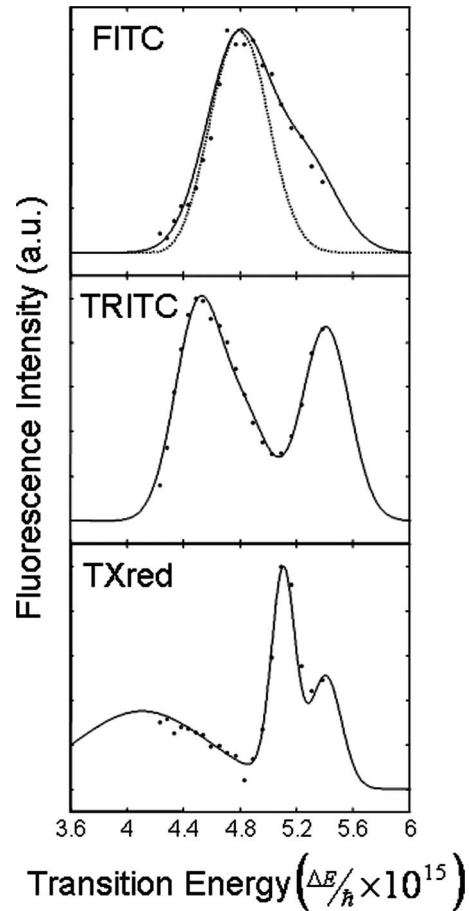


**Fig. 1** Two-photon photoluminescence excitation spectra of FITC, TRITC, and TXred (points). Sum of Gaussians was used to fit the molecular lineshapes (solid lines). Two-photon excitation spectrum of sub-10-fs pulse is shown for reference (dotted line in FITC panel).

Fig. 1). These lineshapes  $\gamma(\omega_0)$  and normalized pulse spectra  $|E(\omega)|^2$  were used to calculate two-photon transition probabilities for each dye as,<sup>7</sup>

$$\Gamma \propto \int_0^\infty \gamma(\omega_0) \left| \int_0^\infty E(\omega_0/2 + \Omega)E(\omega_0/2 - \Omega)d\Omega \right|^2 d\omega_0, \quad (2)$$

where  $\hbar\omega_0$  is the transition energy. Equation (2) follows from second-order, time-dependent perturbation theory, assuming pulsed, nonresonant two-photon excitation and ignoring, for example, strong field effects that could arise from tight focusing. Thus, it is assumed that the two-photon transition probabilities are proportional to the measured TPEF signal.

The TPEF for each dye was measured as a function of pulse duration using two Ti:Al<sub>2</sub>O<sub>3</sub> oscillators (Micra, Coherent and Synergy, Femtolasers). Six pulse durations were generated by Micra centered at 800 nm with FWHM tunable from 10 to 100 nm using an intracavity aperture. To maintain consistent intensity, a beam expander was used to match beam size in all experiments with the two laser systems. A quartz cuvette with a 0.5-mm-path length (NSG Precision Cells) was matched to the depth of focus of the laser beam (50-mm focal

length planoconvex lens) to minimize dispersion from dye solutions. Dispersion was compensated with a prism pair (Short Pulse Option, Coherent) and methods described previously using a spatial light modulator (SLM-256, CRI) and a 10- $\mu\text{m}$ -thick  $\beta$ -barium borate (BBO) type I crystal<sup>8</sup> (Silhouette, Coherent). The spectrometer also measured second-harmonic generation (SHG) intensity from the BBO crystal as a frequency-invariant second-order signal.

Three pulse durations were generated by the Synergy centered at 780 nm (120 nm FWHM) by adding interference bandpass filters (40 and 60 nm bandwidth, CVI Laser) to the beam path. Dispersion compensating mirrors ( $-30 \text{ fs}^2$  per bounce) and a pair of fused silica wedges ( $36 \text{ fs}^2/\text{mm}$ ) were used to compensate chirp from all the transmissive optics including the 1.25-mm-thick cuvette wall in the beam path. Interferometric autocorrelations were monitored to ensure that the pulses were nearly transform limited. The parabolic mirror (50-mm focal length) focused the beam on the sample. The signal from a GaAsP photodiode (PD), which has a frequency-invariant second-order response,<sup>9</sup> was collected in analogy to SHG. To avoid strong field effects from tight focusing, the excitation power for the experiments was below 20 mW.

This same experimental configuration was used to measure TPEF spectra of FITC and TXred solutions and GaAsP PD signal excited by linearly chirped pulses from the Synergy. Linear chirp was added by inserting glass into the beam path.<sup>10</sup>

Introducing dispersion temporally broadens the pulse, reducing peak intensity and two-photon excitation efficiency.<sup>2-4</sup> Two-photon transition probabilities were calculated as a function of linear chirp  $\Phi''$  using the excitation pulse shapes. Linear chirp was introduced to the electric field profiles through an additional phase term,<sup>11</sup>

$$E(\omega) = E_0(\omega - \omega_c) \exp\left[i\frac{\Phi''}{2}(\omega - \omega_c)^2\right], \quad (3)$$

where  $\omega_c$  is the center frequency. The field in Eq. (3) was used to calculate the effect of linear chirp on two-photon excitation spectra and two-photon transition probabilities [c.f., Eqs. (1) and (2)] as well as interferometric autocorrelations, which were compared with those measured experimentally and used to estimate pulse durations.<sup>12,13</sup>

### 3 Results

Transition probabilities for the three dyes and SHG intensity were calculated as a function of Gaussian pulse width centered at 800 nm to understand how it would be expected to vary with incident transform-limited pulse duration, as shown in Fig. 2 (points). A frequency-invariant response function was used to calculate SHG [i.e.,  $\gamma(\omega) \rightarrow \gamma$  in Eq. (2)]. Logarithmic plots of calculated transition probabilities for the three dyes and SHG intensity using experimental pulse spectra are also shown in Fig. 2 (circles). The plots for each dye are offset for clarity. Solid lines with a slope of  $-1$  are shown for reference. The pulse durations were calculated as the FWHM of the transform-limited pulses. Transition probabilities and

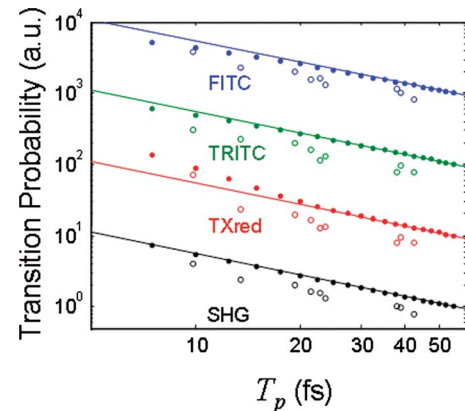


**Fig. 2** Logarithmic plot of calculated transition probabilities for FITC, TRITC, TXred and SHG using Gaussian (points) and experimental pulse spectra (circles). Curves for each dye are offset for clarity. Solid lines with slope of  $-1$  are shown for reference.

SHG intensities calculated for Gaussian and experimental pulse spectra were not identical because of differences in pulse shape.<sup>1</sup>

For sufficiently narrow pulse spectra, the two-photon transition probability as a function of pulse duration should follow  $1/T_p$  relationship. This was observed for the three dyes with Gaussian pulse durations,  $T_p \geq 40 \text{ fs}$ . These pulse durations are typically used for NLOM and have excitation spectra sufficiently narrow to interact with a nearly uniform TPA cross section. Deviation begins to occur for shorter pulses having broader bandwidths; these deviations from  $1/T_p$  behavior were specific to each dye and reflected the relative overlap of molecular 2PES and pulse two-photon excitation spectra. For FITC and TRITC, shorter excitation pulses deviated to lower transition probabilities whereas, for TXred, it deviated toward higher transition probabilities. A frequency invariant response function was used to calculate SHG intensity and therefore varied as  $1/T_p$  over the entire pulse duration range. This behavior reflects the interaction of each individual 2PES with excitation pulses centered at 800 nm.

The calculated transition probabilities for FITC, TRITC, TXred, and SHG as a function of pulse duration when using experimental pulse spectra (circles, Fig. 2) follow the general trends established with Gaussian pulse shapes. Differences in transition probabilities between experimental and Gaussian pulses reflect differences in spectral shape and in central wavelength (800 and 780 nm for Micra and Synergy pulse spectra, respectively).

Dye specific deviations from  $1/T_p$  behavior observed in Fig. 2 as a function of pulse duration suggest that the relative widths (and central frequencies) of excitation spectra  $T(\omega)$  and molecular TPA cross sections  $\gamma(\omega)$  jointly determine the maximum achievable fluorescence intensities for NLOM. To further investigate this phenomenon, transition probabilities were calculated as a function of the transform-limited Gaussian pulse duration and molecular TPA linewidth. In this calculation, the molecular TPA line shapes  $\gamma(\omega)$  had a Gaussian profile and were centered at the same central frequency as the pulse excitation spectra. The results are shown on a logarithmic plot in Fig. 3. The pulse duration is normalized by the temporal width of the Fourier transform of the molecular TPA

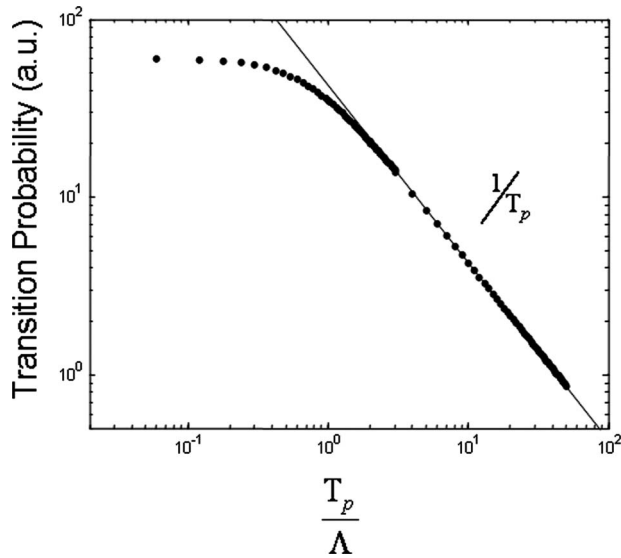


**Fig. 3** Calculated transition probability as a function of transform limited pulse width  $T_p$  normalized to molecular spectral linewidth  $\Lambda$  (see text). A solid line with slope of  $-1$  is shown for reference.

lineshape,  $\Lambda$ , which reflects the time response or dephasing time of the molecule. Note that as the dephasing time  $\Lambda$  increases, the Gaussian lineshape  $\gamma(\omega)$  decreases in spectral width. For reference, a solid line is shown with a slope of  $-1$ . The logarithmic plot in Fig. 3 shows that the transition probability begins to deviate from  $1/T_p$  behavior as  $T_p/\Lambda$  approaches unity, where the pulse spectral width approaches that of the TPA lineshape. As  $T_p/\Lambda$  decreases from unity, the use of shorter pulse durations yields diminishing returns and exhibits asymptotic behavior in the limit where  $T_p/\Lambda < 0.1$ .

Previous studies have characterized TPEF and SHG as a function of pulse duration by introducing dispersion to broaden the temporal width while maintaining the pulse spectrum (scheme 1).<sup>2,4</sup> Although exhibiting a similar  $1/T_p$  relationship, the dependence of TPEF and SHG on chirped pulse duration by the addition of dispersion is characteristically different from what was predicted from our calculations using transform-limited pulses (Figs. 2 and 3). The dependence of TPEF (of FITC and TXred) and SHG (GaAsP PD) on chirped pulse duration was measured by the addition of glass to the beam path of sub-10-fs pulses. Two-photon signal (TPEF and SHG) intensity is shown on a logarithmic plot in Fig. 4 (data points) as a function of linear chirp, normalized to the square of transform-limited pulse duration  $\Phi''/T_p^2$ . Also in Fig. 4, two-photon signals were calculated using Eq. (2) with the addition of a phase term to the sub-10-fs pulse electric field [Eq. (3)] and shown as reference (solid line). Only one reference line is shown because it was found to be independent of molecular 2PES and reproduces the behavior of the experimental data. The agreement between experimental results and calculations resulted from normalizing the data to their respective transform-limited values ( $\Phi''=0$ ); no “fitting” routine was applied. Experimental results and calculations were independent of molecular response—the exhibited behavior reflects dispersion and its effects on pulse peak power and its two-photon excitation—and show that  $1/T_p$  behavior will be

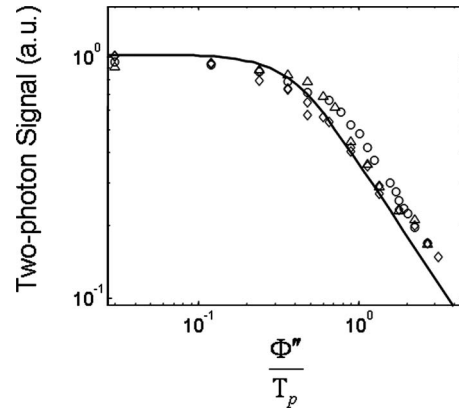


**Fig. 4** Logarithmic plot of two-photon signal for FITC (circles), TXred (triangles), and GaAsP photodiode (diamonds) as a function of linear chirp to broadband laser (FWHM  $\sim 120$  nm, Synergy) and calculated transition probability as a function of linear chirp on the pulse spectrum (solid line).

realized only when  $\Phi''/T_p^2 > 1$  even in the ideal limit of frequency independent response, where  $\gamma(\omega) \rightarrow \gamma$ .

Measurements of two-photon signal as a function of transform limited pulse duration are shown on the logarithmic plot in Fig. 5 (crosses) for the three dyes, BBO crystal, and GaAsP PD. (Hereafter, SHG in BBO crystal and two-photon signal from GaAsP PD will be referred to as SHG.) Each data set acquired using the Micra and Synergy (see Sec. 2) was scaled by a constant to best fit calculated values (circles). With simple scaling, it was observed that the experimental measurements of TPEF and SHG were in fair agreement with the calculated two-photon transition probabilities. For example, measured signal enhancement ratios of sub-10- versus 23-fs pulses from Synergy were 1.77, 2.42, 2.99, and 2.62 compared with the calculated enhancement ratios of 2.28, 2.65, 5.49, and 2.64 for FITC, TRITC, TXred, and SHG, respectively. The error in these measurements was approximately  $\pm 5\%$  for each data point.

The difference between measuring two-photon signal dependence on pulse duration using chirped (scheme 1) and transform-limited pulses (scheme 2) is highlighted in Fig. 6

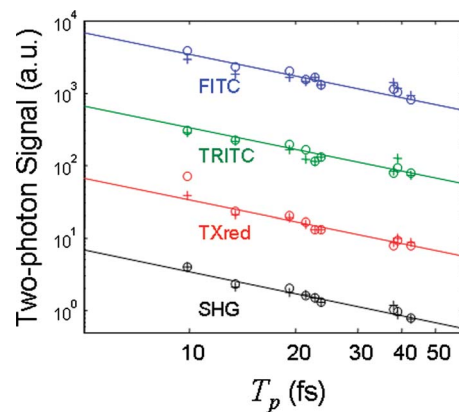


**Fig. 5** Logarithmic plot of calculated (circles) and experimental two-photon excited fluorescence for FITC, TRITC, TXred, and SHG (crosses).

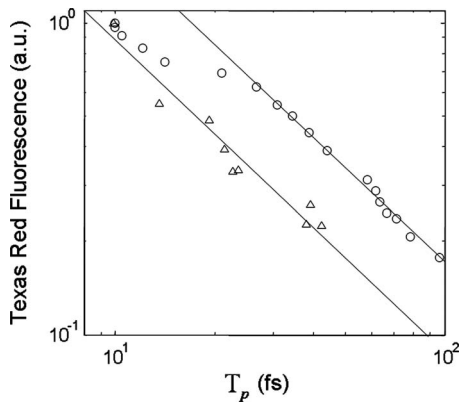


**Fig. 6** Logarithmic plot of two-photon excited fluorescence intensity from TXred using chirped (circles) and transform-limited pulses (triangle).

for TXred. (The same trends are exhibited regardless of the choice of dye or SHG.) Solid lines with a slope of -1 are shown for reference. The data sets from the two measurement schemes are normalized to the common transform limited sub-10-fs data point. For chirped pulses (scheme 1), TXred TPEF shows  $1/T_p$  dependence for  $T_p \geq 30$  fs ( $\Phi''/T_p^2 > 1$ , see Fig. 4) and deviates for shorter pulse durations. This trend represents deviation from  $1/T_p$  behavior due to the effect of chirp (or phase distortion) on pulse two-photon excitation and occurs irrespective of the sample. Indeed, using transform-limited pulses (scheme 2), experimental results show that TXred TPEF could be well approximated by  $1/T_p$  dependence down to sub-10-fs pulse duration. It is also observed that for all pulse durations longer than sub-10-fs, TXred TPEF is higher for chirp broadened sub-10-fs pulses compared with transform limited pulses of the same temporal duration (but of narrower bandwidths).

## 4 Discussion

This study compares and contrasts the measurements of TPEF dependence on pulse duration by introducing dispersion to a short pulse (scheme 1) and by using transform-limited (time-bandwidth product minimized) pulses (scheme 2). Previous studies have characterized TPEF (as well as SHG) as a function of chirped pulse duration and measured a dependence inconsistent with  $1/T_p$  relationship as the transform limit was approached.<sup>2,4</sup> Our experimental results and calculations reveal that chirped pulse measurements (scheme 1) probe a different physical phenomenon. Introducing dispersion or spectral phase only changes the relative arrival times of the pulse frequency components at the interaction volume. Dispersion is known to broaden the pulse duration and reduce peak power.<sup>14</sup> The result is that the measure of the two-photon signal as a function of chirp reflects the effects of phase on the pulse two-photon excitation spectrum irrespective of the molecule with which it interacts. Even in the ideal case of frequency-independent molecular response, i.e.,  $\gamma(\omega) \rightarrow \gamma$ , the  $1/T_p$  relationship will be realized only when  $\Phi''/T_p^2 > 1$ , where only degenerate contributions to the pulse two-photon excitation spectrum remain [see Eq. (1)]. Our results are consistent with and, in fact, extend previous work that character-

ized TPEF dependence on (chirped) pulse duration.<sup>2,4</sup> Using chirped 12-fs pulses, TPEF dependence was shown to deviate from  $1/T_p$  behavior for pulse durations below 50 fs, consistent with our prediction<sup>4</sup> of  $\Phi''/T_p^2 \leq 1$  ( $\sim 35$  fs) from Fig. 4. In previous work characterizing TPEF dependence using chirped 60-fs pulses, the authors noted “significant deviation” from  $1/T_p$  behavior for pulse durations below 90 fs as the transform limit was approached and, thus, omitted those data.<sup>2</sup> In addition, note that the 90-fs pulse width measurement was made before the beam expander and objective lens, suggesting that the actual pulse duration at the sample was temporally broader than reported. Our results predict deviations from  $1/T_p$  behavior should have been observed for durations less than  $\sim 180$  fs, where  $\Phi''/T_p^2 \leq 1$ .

TPEF dependence on pulse duration is measured when using transform-limited pulses (scheme 2) and would be expected to depend on molecular TPA cross section in the limit where  $T_p/\Lambda$  approaches unity, i.e., in the limit where TPA is no longer invariant over the entire pulse excitation spectrum. Our calculations based on Gaussian pulse shapes and measured 2PES of the dyes suggest that the shortest experimental pulse durations used in this study should be beyond the  $1/T_p$  limit, albeit with relatively small sample dependent deviations (see Fig. 2). However, deviations from  $1/T_p$  behavior in our measurements were not obvious because the pulse shapes used were not identical and the two Ti:Al<sub>2</sub>O<sub>3</sub> oscillators from which the data sets were acquired were centered at 780 and 800 nm (detuned by 2.5% compared with  $\Delta\lambda(\text{FWHM})/\lambda$  of 15%). Our measurements of two-photon signal dependence on pulse duration were comparable to transition probability calculations. The greatest deviation was observed in the sub-10-fs data points for TXred. There are several possible reasons for discrepancies between experimental and calculated signal levels including residual chirp in the pulses, differences in focal volume that arise from different pulse spectra and error in the measured 2PES of the dyes. Residual chirp would be particularly acute for measurements of TPEF in TXred because of its sharp 2PES profile on the high energy edge of the sub-10-fs pulse excitation spectrum (see Fig. 1).

Transition probabilities calculated for the three dyes lend credence to the idea that the use of ultrashort pulses not only enhances TPEF signal, but facilitates simultaneous excitation of multiple fluorophores for multicolor molecular imaging with NLOM. The maximum in TRITC 2PES was found for a narrowband, 170-fs pulse with its central wavelength tuned to 840 nm. If the transition probability of TRITC was calculated for the sub-10- and 170-fs pulses tuned to 840 nm, the fluorescence intensity would be enhanced by a factor of 9.4 for the ultrashort pulse. Similarly for TXred, the sub-10- compared to 170-fs pulses tuned to the 2PES maximum (740 nm) was calculated to have a higher transition probability (and, hence, fluorescence intensity) by a factor of 4.6. These limited examples suggest that ultrashort pulses can enhance fluorescence intensity even for 2PES line shapes not well centered on its spectrum compared with narrowband, ultrafast pulses tuned for maximum (fluorescence) signal and enable intravital multiple molecular imaging *in situ*.<sup>15</sup>

With commercial Ti:Al<sub>2</sub>O<sub>3</sub> oscillators generating pulse durations that span an order of magnitude, the question has been posed previously, concerning what is the optimal pulse

duration for TPEF microscopy.<sup>5</sup> Assuming well-behaved molecular (Gaussian) TPA and Gaussian pulse shapes, our calculations show that asymptotic behavior is exhibited for pulse durations with spectral widths  $\sim 10$  times molecular line-widths (see Fig. 3). Special attention should be paid to the direct comparison of two-photon signal (TPEF or SHG) generated using a chirp-broadened pulse with a transform limited pulse of the same temporal duration, as presented in Fig. 6. The experimental results and calculations show that two-photon signal is higher for a chirp-broadened 10-fs pulse than for a transform-limited pulse of the same temporal duration. For example, a 10-fs pulse broadened to a 100-fs duration will generate more two-photon signal when compared with a transform-limited 100-fs pulse. On the surface, this result appears counterintuitive in light of the fact that (nonresonant) TPEF signal is maximized when using that spectrum's transform-limited (or minimum time duration) pulse.<sup>2-4</sup> In the case of Fig. 6, the pulses for each duration (greater than 10 fs) differ in both spectral bandwidth and phase, with the pulse of greater bandwidth generating more two-photon signal. For practical purposes, note that the susceptibility of laser pulses to dispersion scales with the square of its bandwidth. Thus, the advantages gained with the use of ultrashort pulses are rapidly eroded without careful dispersion compensation. This signal enhancement will also depend on the molecular response, decreasing for  $T_p/\Lambda \leq 2$ , as shown in Fig. 3.

NLOM is touted for its ability to render thin, microscopic images from within thick, intact tissues because of its increased imaging depth and reduced susceptibility to photobleach and damage. NLOM is particularly sensitive to the extracellular matrix, providing an experimental platform on which to study cell-matrix interactions at microscopic length scales. However, these attributes are tempered by the inability of NLOM to probe beyond superficial layers in most biological tissues because of light scattering. It has been suggested that imaging depth could be increased with the use of shorter duration pulses because of enhanced signal generation.<sup>4,5</sup> However, this advantage may be mitigated by increasing pulse energies for longer duration pulses. Indeed, NLOM images acquired as deep as 1 mm from within highly scattering biological tissue have been reported using narrowband,  $\sim 100$ -fs pulses.<sup>16</sup> Ultimately, the limit to depth of imaging is determined by deterioration in SNR from surface background fluorescence.<sup>17</sup>

We submit that the susceptibility of ultrashort pulses to dispersion may be used to suppress surface background fluorescence and extend the imaging depth of NLOM. Assuming dispersion of biological tissue can be approximated by that of water,  $\sim 100$  fs<sup>2</sup> of chirp is imparted by 4 mm of water.<sup>10</sup> For dispersion-compensated pulses at the focus 1 mm deep,  $\Phi''/T_p^2$  at the surface is 0.0025, 0.25, and 0.51 for 100-, 10-, and 7-fs pulses, respectively. For 7-fs pulses, two-photon signal generation is diminished by  $\sim 30\%$  at the surface and would be further diminished with increasing depth (see Fig. 4).

## 5 Conclusions

The use of chirped and transform-limited pulses was compared and contrasted in the characterization of TPEF and SHG dependence on pulse duration. When using chirped pulses to

characterize TPEF and SHG dependence, experimental data show and calculations predict deviation from  $1/T_p$  behavior as pulse duration approached its transform limit, independent of the molecular response. The use of chirped pulses characterizes the effects of dispersion on the nonlinear excitation spectrum without revealing the pulse duration dependence of two-photon processes. In contrast, transform-limited pulses with durations as short as sub-10-fs showed a molecularly dependent response with little deviation from the expected  $1/T_p$  behavior. Calculations confirm the validity of experimental observations and predict a transition in TPEF pulse duration dependence from  $1/T_p$  to asymptotic behavior for decreasing (ultrashort) pulse durations. A direct comparison of TPEF using chirped and transform-limited pulses shows that the chirp broadened pulse with a shorter transform-limited pulse width (and broader spectrum) will generate a higher signal than a transform-limited pulse of the same temporal duration (but narrower spectrum). These results suggest that, as a design parameter, ultrashort pulse durations will enhance the performance of NLOM systems.

## Acknowledgments

We thank Adam M. Larson and Haribhaskar Balasubramanian for assisting with the experiments, Coherent for demonstration of the Micra, Short Pulse Option, and Silhouette, and Microscopy & Imaging Center at Texas A&M University for use of the Synergy. This work was supported by the National Science Foundation, Faculty Early Career Development (CAREER) Award (A.T.Y.).

## References

1. C. J. Bardeen, V. V. Yakovlev, J. A. Squier, K. R. Wilson, S. D. Carpenter, and P. M. Weber, "Effect of pulse shape on the efficiency of multiphoton processes: implications for biological microscopy," *J. Biomed. Opt.* **4**(3), 362–367 (1999).
2. C. Xu and W. W. Webb, "Measurement of two-photon excitation cross sections of molecular fluorophores with data from 690 to 1050 nm," *J. Opt. Soc. Am. B* **13**(3), 481–491 (1996).
3. G. McConnell, "Improving the penetration depth in multiphoton excitation laser scanning microscopy," *J. Biomed. Opt.* **11**(5), 054020 (2006).
4. S. Tang, T. B. Krasieva, Z. Chen, G. Tempea, and B. J. Tromberg, "Effect of pulse duration on two-photon excited fluorescence and second harmonic generation in nonlinear optical microscopy," *J. Biomed. Opt.* **11**(2), 020501 (2006).
5. P. Xi, Y. Andegeko, L. R. Weisel, V. V. Lozovoy, and M. Dantus, "Greater signal, increased depth, and less photobleaching in two-photon microscopy with 10 fs pulses," *Opt. Commun.* **281**(7), 1841–1849 (2008).
6. N. Dudovich, B. Dayan, S. M. Faeder Gallagher, and Y. Silberberg, "Transform-limited pulses are not optimal for resonant multiphoton transitions," *Phys. Rev. Lett.* **86**(1), 47–50 (2001).
7. D. Meshulach and Y. Silberberg, "Coherent quantum control of multiphoton transitions by shaped ultrashort optical pulses," *Phys. Rev. A* **60**(2), 1287–1292 (1999).
8. K. A. Walowicz, I. Pastirk, V. V. Lozovoy, and M. Dantus, "Multiphoton intrapulse interference. I. Control of multiphoton processes in condensed phases," *J. Phys. Chem. A* **106**(41), 9369–9373 (2002).
9. J. K. Ranka, A. L. Gaeta, A. Baltuska, M. S. Pshenichnikov, and D. A. Wiersma, "Autocorrelation measurement of 6-fs pulses based on the two-photon-induced photocurrent in a GaAsP photodiode," *Opt. Lett.* **22**(17), 1344–1346 (1997).
10. A. G. Van Engen, S. A. Diddams, and T. S. Clement, "Dispersion measurements of water with white-light interferometry," *Appl. Opt.* **37**(24), 5679–5686 (1998).

11. J.-P. Foing, M. Joffre, J.-L. Oudar, and D. Hulin, "Coherence effects in pump-probe experiments with chirped pump pulses," *J. Opt. Soc. Am. B* **10**(7), 1143–1148 (1993).
12. J.-C. M. Diels, J. J. Fontaine, I. C. McMichael, and F. Simoni, "Control and measurement of ultrashort pulse shapes (in amplitude and phase) with femtosecond accuracy," *Appl. Opt.* **24**(9), 1270–1282 (1985).
13. K. Naganuma, K. Mogi, and H. Yamada, "General method for ultrashort light pulse chirp measurement," *IEEE J. Quantum Electron.* **25**(6), 1225–1233 (1989).
14. A. E. Siegman, *Lasers*, University Science Books, Sausalito, CA (1986).
15. A. T. Yeh, H. Gibbs, J.-J. Hu, and A. M. Larson, "Advances in nonlinear optical microscopy for visualizing dynamic tissue properties in culture," *Tissue Eng. B Rev.* **14**(1), 119–131 (2008).
16. P. Theer, M. T. Hasan, and W. Denk, "Two-photon imaging to a depth of 1000  $\mu\text{m}$  in living brains by use of a Ti:Al<sub>2</sub>O<sub>3</sub> regenerative amplifier," *Opt. Lett.* **28**(12), 1022–1024 (2003).
17. P. Theer and W. Denk, "On the fundamental imaging-depth limit in two-photon microscopy," *J. Opt. Soc. Am. A* **23**(12), 3139–3149 (2006).